On the Electronic Structure of Bismuth and Its Dilute Alloys

On the Electronic Structure of Bismuth and Its Dilute Alloys*

Tadao FUKUROI, Yoshio MUTO, Yoshitami SAITO**,
Kunihide TANAKA and Tetsuo FUKASE

(Received August 18, 1966)

Synopsis

We studied the quantum oscillatory phenomena which were observed at 1.2～4.2°K in the de Haas-van Alphen effect, the magneto-acoustic attenuation, and the Shubnikov-de Haas effect of pure bismuth and its alloys doped with a small amount of tin, tellurium, antimony, arsenic or manganese. Our results obtained in this study with respect to pure bismuth, are in good agreement with the results of the other investigators. From the change of the periods of Shubnikov-de Haas oscillations in dilute bismuth alloys, we discussed the electronic band structure in the higher and lower energy parts than the Fermi level of pure bismuth, and could conclude that the Cohen's model gives a better approximation for the comprehension of the results.

I. Introduction

Since 1959, we have carried out the experimental studies on the electrical properties of bismuth, antimony and their alloys. In this series of works are included the investigations on the galvanomagnetic effects of bismuth[1-3] and antimony[4], the semiconducting properties of bismuth-antimony alloys[5,6], some electrical properties of dilute alloys of bismuth with tin, tellurium, and arsenic[7], the de Haas-van Alphen effects of antimony[8] and bismuth[9], and the magneto-acoustic attenuations of bismuth[10] and antimony[11]. In the present paper, our investigations on the electronic structure of bismuth and its alloys, by using the quantum oscillatory phenomena, are summarized.

Up to date the Fermi surface of bismuth has been extensively studied by

---

* The **1274th** report of the Research Institute for Iron, Steel and Other Metals.

** Present address: Department of Applied Physics, Faculty of Engineering, Tohoku University.

(1) S. Mase and S. Tanuma, J. Phys. Soc. Japan, **14** (1959), 1644.
(2) S. Mase and S. Tanuma, Sci. Rep. RITU, **A12** (1960), 35.
(3) K. Tanaka, S. Tanuma and T. Fukuroi, Sci. Rep. RITU, **A13** (1961), 67.
(4) K. Tanaka, Sci. Rep. RITU, **A16** (1964), 123.
(5) S. Tanuma, J. Phys. Soc. Japan, **14** (1959), 1246; **16** (1961), 2349, 2354.
(6) S. Tanuma, K. Tanaka, T. Mamiya and T. Fukuroi, *High Magnetic Field* (1961), Wiley & Sons, p. 534.
(7) K. Tanaka, J. Phys. Soc. Japan, **29** (1965), 1374, 1633.
(8) Y. Saito, J. Phys. Soc. Japan, **18** (1963), 452; **19** (1964), 1319.
(9) Y. Saito, J. Phys. Soc. Japan, **18** (1963), 1845.
(10) T. Fukase and T. Fukuroi, to be published.
(11) T. Fukase and T. Fukuroi, J. Phys. Soc. Japan, **21** (1966), 814 and *The Physics of Semiconductors*; (International Conf. on Semiconductors, 1966.), 751.

means of the de Haas-van Alphen effect[12]-[15], the galvanomagnetic effect[16,17,18], the magneto-thermal oscillations[19], the ultrasonic attenuation[20-23], the magneto-striction[24], the cyclotron resonance[25]-[28], the surface resistance measurements[29], the magneto-reflection[30] and so forth. According to a usual model on the electronic structure of bismuth obtained by Shoenberg[13] and Brandt[14], three electron ellipsoids are located in the three-fold symmetry with $\pm 120°$ rotation around the trigonal axis of a crystal, and a hole ellipsoid lies on the trigonal axis.

The Fermi level of bismuth can be changed by an addition of a small amount of electron donor or acceptor, such as tellurium or tin[7,12], without affecting the crystal potential. As the impurity concentration increases, the electronic structure of bismuth below or above the Fermi level is to be revealed. On the other hand, the addition of elements such as antimony and arsenic, which belongs to the same column as bismuth in the periodic table, gives rise to a change in the lattice parameters, modifying the energy band structure keeping the electron and the hole concentrations in an equivalence[5]. However, the influence on the band structure of bismuth due to the addition of transition metal is not yet ascertained. For instance, inasmuch as the electrical resistance of bismuth alloys containing a small amount of manganese decreases with decreasing temperature below 4.2°K, it might be expected that manganese atoms in bismuth have no localized moment[32]. It would be desirable to study the electronic structure in such alloys.

In this paper, the de Haas-van Alphen effect up to 25 kOe, the magneto-acoustic attenuation up to 18 kOe, and the Shubnikov-de Haas effect up to 18 kOe are investigated with respect to pure bismuth single crystals at liquid helium temperatures.

(12) D. Shoenberg and M.Z. Uddin, Proc. Roy. Soc. London, **A 156** (1936), 701.
(13) D. Shoenberg, Proc. Roy. Soc. London, **158** (1938), 341: Phil. Trans. Roy. Soc., **A 245** (1952), 1.
(14) N.B. Brandt, A.E. Dubrovskaya and G.A. Kytin, Sov. Phys. JETP, **10** (1960), 405; **11** (1960), 975.
(15) D. Weiner, Phys. Rev., **125** (1962), 1226.
(16) L.S. Lerner, Phys. Rev., **127** (1962), 480.
(17) S. Mase, S. von Molnar and A.M. Lawson, Phys. Rev., **127** (1962), 1030.
(18) M.C. Steel and J. Babiskin, Phys. Rev., **98** (1955), 359.
(19) J.E. Kunzler, and F.S.L.Hsu, *Fermi Surface* (1960), Wiley & Sons, p. 88: J.E. Kunzler. W.S. Boyle, F.S.L.Hsu Phys. Rev. **128**, (1962), 1084.
(20) D.H. Reneker, Phys. Rev., **115** (1959), 303.
(21) A.P. Korolyuk, Sov. Phys. Solid State, **5** (1964), 2433.
(22) A.M. Toxen and S. Tansal, Phys. Rev., **137** (1965), A211.
(23) A.P. Korolyuk, Sov. Phys. JETP, **22** (1966), 701.
(24) B.A. Green and B.S. Chandrasekhar, Phys. Rev. Letters, **11** (1963), 331.
(25) J.E. Aubrey and R.G. Chambers, J. Phys. Chem. Solids, **3** (1957), 128.
(26) J.K. Galt, W.A. Yager, F.R. Merrit, B.B. Cetlin and H.W. Dail, Phys. Rev., **100** (1955), 748.
(27) Y.H. Kao, Phys. Rev., **129** (1963), 1122.
(28) Y.H. Kao, R.D. Brown, III and R.L. Hartman, Phys. Rev., **136** (1964), A858.
(29) G.E. Smith, Phys. Rev., **115** (1959), 115.
(30) R.N. Brown, J.G. Mavroides and B. Lax, Phys. Rev., **129** (1963), 2055.
(31) A.L. Jain, Phys. Rev., **121** (1961), 387.
(32) H. Kitagawa, Y. Muto and T. Fukuroi, J. Phys. Soc. Japan, **21** (1966), 2088.

The periods of quantum oscillations observed in every principal plane ascribable to the Fermi surface of electron or hole are compared with each other and with the results of many other investigators.

Further the Shubnikov-de Haas oscillations in bismuth alloys which contain small concentrations of tin, tellurium, antimony, arsenic, or manganese are investigated by means of a special technique described later. In addition to the periods responsible for the usual electron ellipsoids, the hole periods are observed in most of the alloys studied. These results are discussed on the basis of the electronic structure of bismuth and its alloys.

II. Experimental procedures

Bismuth of the quoted purity of 99.9999%, purchased from Asahi Metal Co. Ltd., was further purified by passing through 30 melting zones. Tin, tellurium, antimony, and arsenic used for alloying had much the same purity. Manganese used for doping was 99.99% in purity, purchased from Johnson Matthey & Co. Ltd. The Czochralski's technique was used for growing a single crystal of pure bismuth. The single crystals of alloys were grown by the Bridgman technique. The crystallographical axes of the specimen were determined by a light figure technique.

Table 1. The concentrations of minor elements and the residual resistance ratio ,i.e. $R_{273°K}/R_{4.2°K}$.

Specimens	Concentration of minor elements in atomic %	$R_{273°K}/R_{4.2°K}$ (I//y-axis)
pure Bi	—	151.3
Bi-Sb:A	0.40	48.03
Bi-Sb:B	1.79	16.99
Bi-As:A	0.017	42.25
Bi-As:B	0.17	20.10
Bi-Te	0.005	5.24
Bi-Sn	0.0018	3.46
Bi-Mn:A	*	56.35
Bi-Mn:B	0.201	13.13
Bi-Mn:C	0.267	16.09
Bi-Mn:D	0.338	9.50

* In Bi-Mn:A, manganese was not analysed chemically but it could be detected spectroscopically.

The specimens for the study of the de Haas-van Alphen effect were cut into pieces from 100 to 200 mg in weight along the desired axial orientation. The specimen used for the magneto-acoustic attenuation measurements was cut and planed by the Servomet spark machine, the dimension of which was $8.73\times10.35\times9.21$ mm^3 measured along the binary, bisectrix, and trigonal axes. The specimens used for Shubnikov-de Haas experiments had the dimension of about $1.5\times1.5\times10$ mm^3 that was cut from the same single crystal which was used for the

magneto-acoustic measurements. The residual resistance ratios of pure bismuth crystals, i.e. the values of $\rho_{273°K}/\rho_{4.2°K}$ are 94.9 for I//x, 151.3 for I//y and 138.3 for I//z, in which I denotes the direction of the current flow. Experiments of the Shubnikov-de Haas effect on bismuth alloys were done only in the case of the electrical current flowing parallel to the bisectrix axis.

The instrument used for the de Haas-van Alphen effect is the same automatic recording torque magnetometer as described in previous papers[8,9]. The voltage proportional to the amount of torque was fed to the Y-axis and the e.m.f. of an n-Ge Hall probe proportional to the magnetic field up to 24 kOe was fed to the X-axis of an X-Y recorder.

The magneto-acoustic attenuation measurements were performed by a usual pulse technique in the frequency range from 15 to 175 Mc/s with a longitudinal acoustic waves. The echo signals which exponentially decayed were led to a logarithmic amplifier through a selective gate and fed to the Y-axis of an X-Y recorder. The magnetic field up to 17.5 kOe was displayed on the X-axis likewise in the de Haas-van Alphen measurements. Quartz transducers were attached on both sides of a rectangular shaped specimen with GE 7031 adhesive. The detailed experimental technique will be published elsewhere[10].

In a measurement of the Shubnikov-de Haas effect, a polycrystalline sample was used for the reference, the resistance of which displayed the similar field dependence without showing oscillations. The difference e.m.f. caused by the magnetoresistance of the single crystal specimen and of the above mentioned reference sample was fed to a D.C. amplifier and led to the Y-axis of an X-Y recorder. The magnetic field up to 17 kOe was displayed on the X-axis as in other measurements. Thus quite small oscillations could be accurately detected.

III. Experimental results

1. de Haas-van Alphen effect of pure bismuth

The crystal orientation determined by means of a light figure technique was further ascertained by measuring the angular dependence of a torque in a fixed magnetic field at room temperatures as shown in Fig. 1. de Haas-van Alphen measurements were done in three principal planes, the typical results of which were given in Fig. 2. de Haas-van Alphen oscillations in a weak field are ascribable to the electron ellipsoids and the oscillations in higher fields above 16 kOe are due to the hole ellipsoid. The splitting which would be attributed to the electron spin can be observed at about 14 kOe[9].

2. Magneto-acoustic attenuation of pure bismuth

A quite sharp tilt effect was observed in a weak magnetic field as described by Reneker[20] and Mase et al.[33] However, the specimen under study displays

(33) S. Mase, Y. Fujimori and H. Mori, J. Phys. Soc. Japan, **21** (1966), 1744.

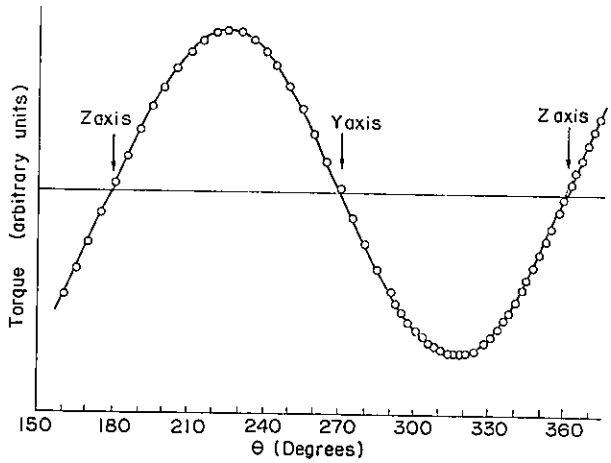

Fig. 1. The angular dependence of a torque at room temperature in the magnetic field of 20.6 kOe. The field is rotated in the bisectrix(y)-trigonal(z) plane of the pure bismuth specimen.

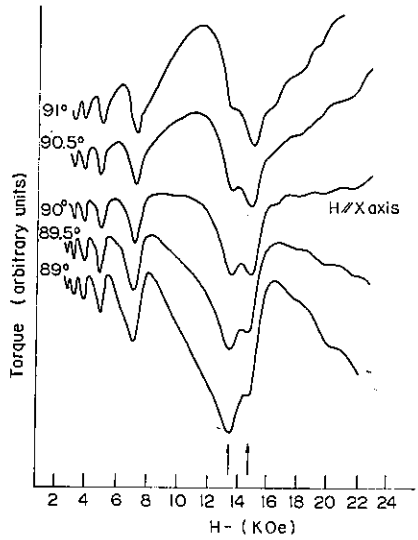

Fig. 2. de Haas-van Alphen oscillations observed at 1.4°K. The magnetic field is nearly parallel to the binary (x) axis in the trigonal-binary plane. Oscillations in the lower field are ascribed to the electron ellipsoid and oscillations in the higher field to the hole ellipsoid. Arrows seen near 14 kOe point the spin splitting due to electrons. (Angles in the figure are measured from the trigonal axis.)

a finer structure in the neighbourhood of $q \perp H$, where q is a propagation vector of the acoustic wave. In Fig. 3 is shown the magneto-acoustic attenuation in the neighbourhood of the trigonal axis in the case of $q \parallel x$ as a function of the angle of the magnetic field orientation. At the angles above 10° from the trigonal axis, curves become nearly flat. Similar characteristics are observed in

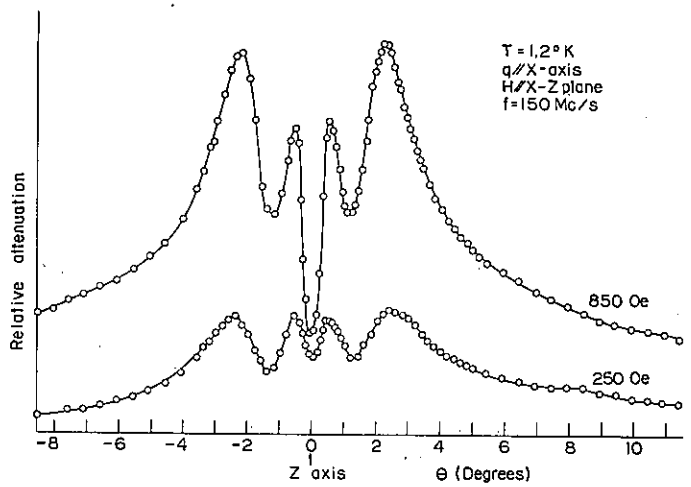

Fig. 3. Ultrasonic attenuation versus θ curves near z axis for the case of q//x at 1.2°K and f=150 Mc/s when the magnetic field was rotated in the trigonal-binary plane.

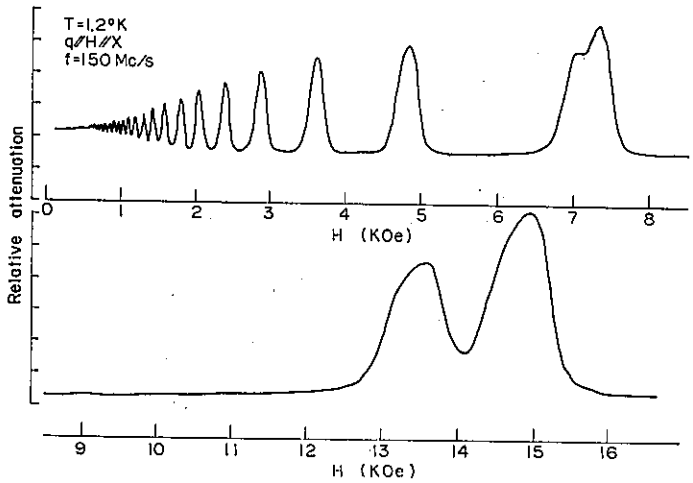

Fig. 4. Ultrasonic attenuation in pure bismuth as a function of magnetic fields in the case of q//H//x at 1.2°K with f=150 Mc/s.

every case of $q \perp H$. By dint of this tilt effect, the relative direction of q and H could be exactly determined. In Figs. 4 and 5 is shown the magneto-acoustic effect in the cases of q//H//x and q//H//z, respectively. The attenuation curve has not a sinusoidal shape but rather a resonance-like one with sharp peaks. This implys that the type of oscillations is a salient feature of the giant oscillations. The oscillations in Fig. 4 is attributed to the electron ellipsoids and the oscillations in Fig. 5 would be due to the hole ellipsoid. It is noticeable that every peak in the

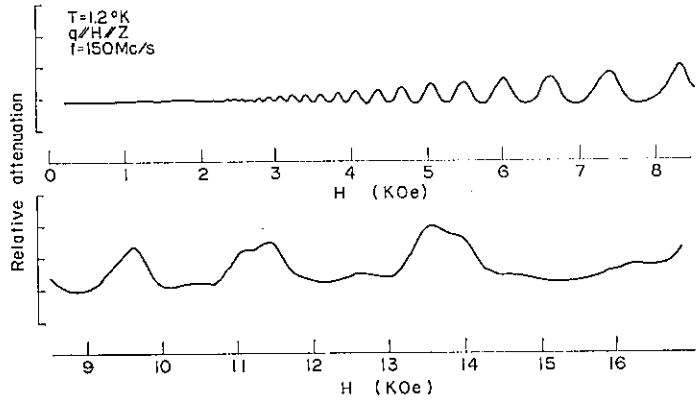

Fig. 5. Ultrasonic attenuation in pure bismuth as a function of magnetic fields in the case of q//H//z at 1.2°K with f=150 Mc/s.

higher field region splits into twin peaks in both figures. This fact would be due to the spin splitting of the Landau levels as described in the de Haas-van Alphen effect.

3. Shubnikov-de Haas effect of pure bismuth

In Fig. 6 are shown the resistance changes in the magnetic field of 16.3 kOe at the liquid nitrogen temperature as a function of the angle between the crystal axis and the field, when the current flowed along the trigonal axis and the

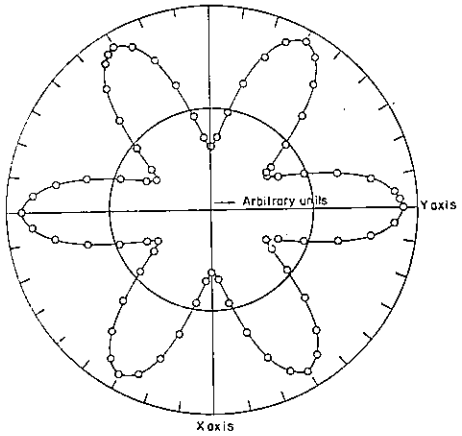

Fig. 6. Voltages proportional to the magnetoresistance as a function of the angle between the bismuth crystal orientation and the field of 16.33 kOe. The current flowed along the trigonal (z) axis and the field was rotated in the binary (x)-bisectrix(y) plane.

field was rotated in the binary-bisectrix plane. Such change of resistance versus magnet setting angle characteristics was also studied when the magnetic field was rotated in the trigonal-binary and the bisectrix-trigonal planes. These results were used for an exact orientation of the crystal axis of the specimens.

A typical example of Shubnikov-de Haas oscillations was shown in Fig. 7, in which the main oscillations would be ascribable to the electron, the small oscillations between 8 and 13 kOe to the hole and a fine structure found near 14 kOe to the electron spin splitting.

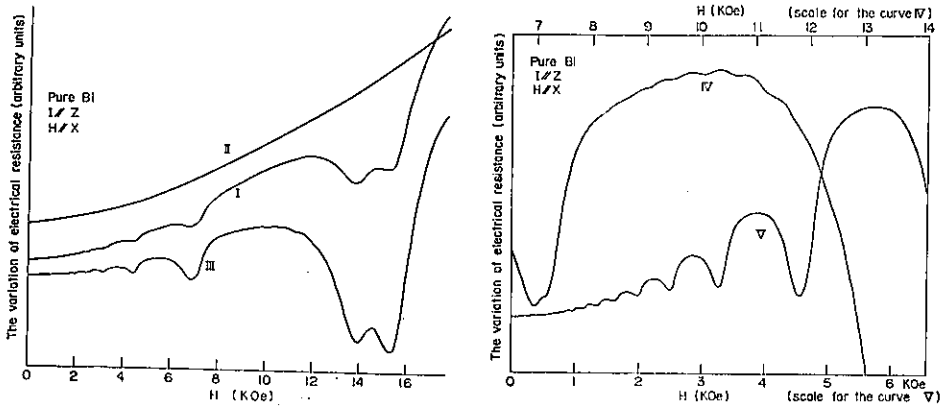

Fig. 7. A typical example of Shubnikov-de Haas measurements.

(a) Curve I is the magnetoresistance of the pure bismuth single crystal when the current flows along the trigonal axis and the magnetic field is parallel to the binary axis. Curve II is the magnetoresistance of polycrystalline bismuth which does not show any oscillatory behavior. Curve III is the observed Shubnikov-de Haas oscillations. This curve is obtained by d.c. amplifying the difference voltage between the curves I and II. Main oscillations in the curve III is attributed to the electrons. A small peak at 14.5 kOe comes from the electron spin splitting. Small oscillations due to the holes can be seen in the range from 8 to 13 kOe.

(b) Oscillations due to holes were further enlarged, as shown in Curve IV, in the above-cited field range by the similar procedure as Curve III. A hump seen at near 7.2 kOe. may also be due to the spin splitting. Curve V is that observed in the lower field range. In Curve V, the oscillations due to electrons can be observed even in the fields below 1 kOe.

From the above experimental data, we could obtain the relationship between the periods of the de Haas-van Alphen type oscillations and the direction of the magnetic field. In Figs. 8, 9, and 10 is shown the angular dependence of periods obtained from the data of the de Haas-van Alphen effect, the magneto-acoustic attenuation, and the Shubnikov-de Haas effect, respectively. In the figures, the open circles can be assigned to the Fermi surface of electron and the full circles to the Fermi surface of hole. These results are in fairly good agreement with the results of other investigators[14,25-28,33].

4. Shubnikov-de Haas effect of several kinds of bismuth alloys

Shubnikov-de Haas oscillations of bismuth alloys listed in Table 1 were studied at 1.2°K, when the magnetic field was rotated in the trigonal-binary plane and the

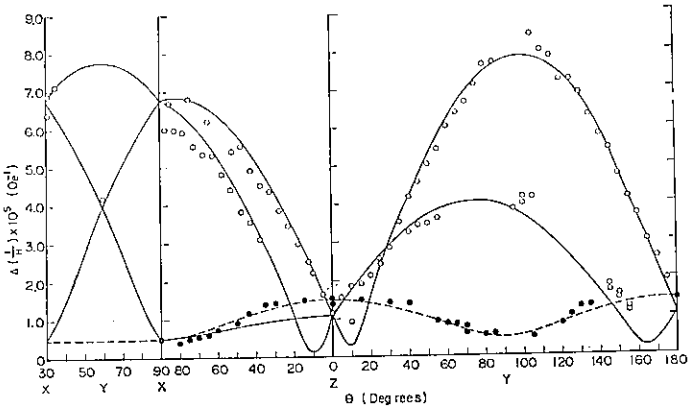

Fig. 8. Angular dependence of the periods of the de Haas-van Alphen effect in pure bismuth. The points denote the observed values. The full curves are obtained with suitable electron parameters and the dotted one with the values replaced by hole parameters.

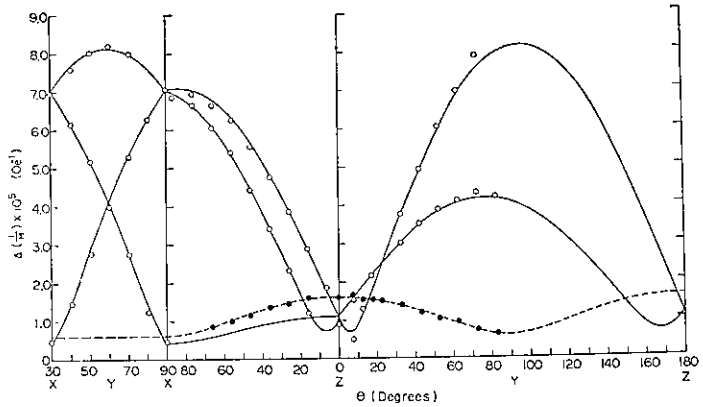

Fig. 9. Angular dependence of the periods obtained from the ultrasonic attenuation in pure bismuth. The curves are obtained by means of least squares fit.

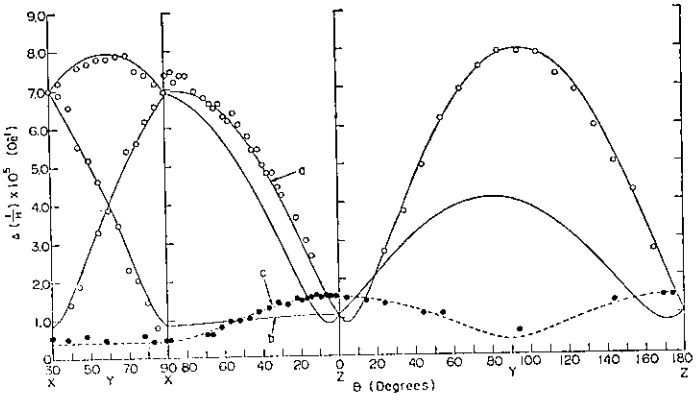

Fig. 10. Angular dependence of the periods obtained from the Shubnikov-de Haas effect in pure bismuth. The curves are obtained by means of least squares fit.

current flow was parallel to the bisectrix axis. Prior to every measurement, the magnetoresistance at a certain magnetic field were measured as a function of the magnetic field orientation chiefly at liquid nitrogen temperature like in Fig. 6 and it was served for an accurate mounting of the specimen.

In Figs. 11 and 12 are shown the Shubnikov-de Haas oscillations of Bi-Sb alloys for the magnetic field along the binary and trigonal axes. The oscillations due to the electron or the hole were observed. Although the alloy specimen Bi-Sb: B contains 1.79 at. % of antimony, it exhibited clear oscillations. In Figs. 13 and 14 are shown the Shubnikov-de Haas oscillations for specimens Bi-As. The Bi-As alloys gave also a similar behavior as the Bi-Sb alloys.

In Fig. 15 is shown the Shubnikov-de Haas effect of the Bi-Te alloy observed

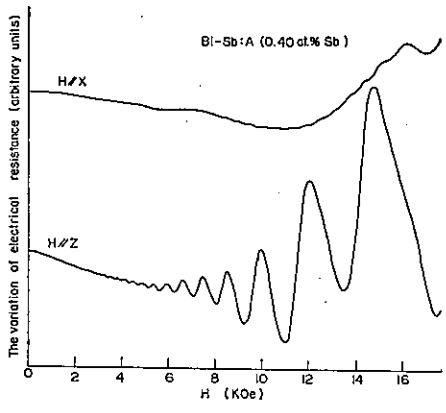

Fig. 11

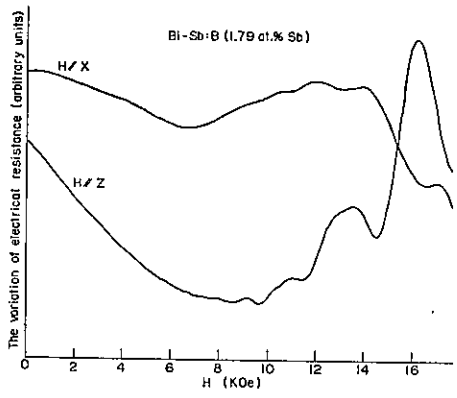

Fig. 12

Fig. 11. Shubnikov-de Haas oscillations of the alloy Bi-Sb:A for H//x and H//z at 1.2°K.
Fig. 12. Shubnikov-de Haas oscillations of the alloy Bi-Sb:B for H//x and H//z at 1.2°K.

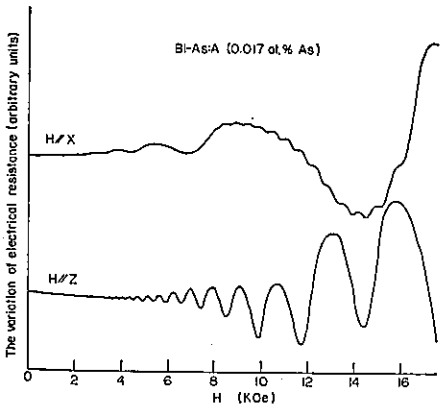

Fig. 13

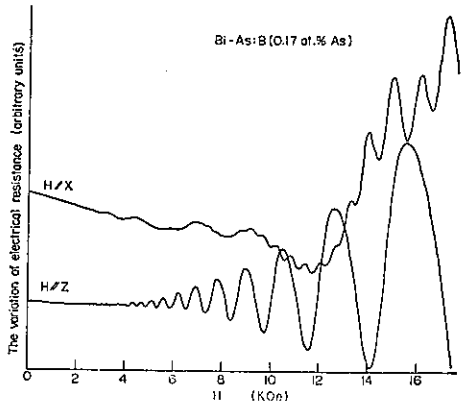

Fig. 14

Fig. 13. Shubnikov-de Haas oscillations of the alloy Bi-As:A for H//x and H//z at 1.2°K.
Fig. 14. Shubnikov-de Haas oscillations of the alloy Bi-As:B for H//x and H//z at 1.2°K.

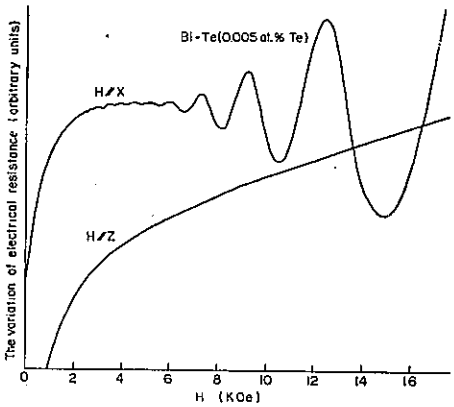

Fig. 15. Shubnikov-de Haas measurements of the alloy Bi-Te for H//x and H//z at 1.2°K. The curve for H//z does not show any oscillatory behavior.

under the magnetic field applied parallel to the binary and the trigonal axis. The oscillation could be observed when the magnetic field was applied parallel to the binary axis, while it could be hardly observed for the field applied parallel to the trigonal axis. In our measurements, for any direction of the magnetic field the amplitude and the period of the oscillation in the Bi-Te alloy were smaller than those in pure bismuth. From the data of the said alloy specimen only one kind of period was analysed and it was assigned to the contribution of an electron band as discussed later.

In Fig. 16 is also shown the Shubnikov-de Haas oscillation of the Bi-Sn alloy for the magnetic field applied parallel to the binary and the trigonal axis. In contrast to the case of the Bi-Te alloy, the oscillations of the Bi-Sn alloy were more remarkably observed when the magnetic field was applied parallel to the trigonal

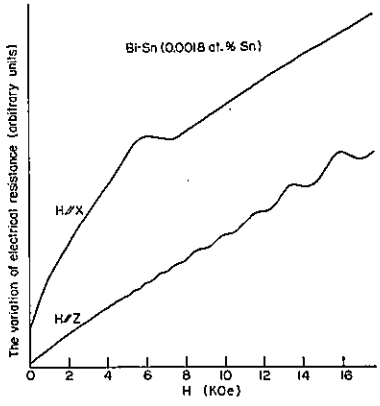

Fig. 16. Shubnikov-de Haas measurements of the alloy Bi-Sn for H//x and H//z at 1.2°K. The curve for H//x shows a unique hump but this cannot be ascribed to the electrons.

axis than to the binary axis, so that we must ascribe the oscillations to the contribution of the different Fermi surface from that in the Bi-Te alloy. From the data of the Bi-Sn alloy specimen under study, two kinds of periods were analysed out, i.e. one of them was ascribable to the Fermi surface of electron and the other to that of hole.

In Fig. 17, the transverse magnetoresistance of the specimen Bi-Mn:A is shown, so far as a clear oscillatory effect, a quite similar one to the pure bismuth*, was observed. In Figs. 18, 19, and 20 are shown the Shubnikov-

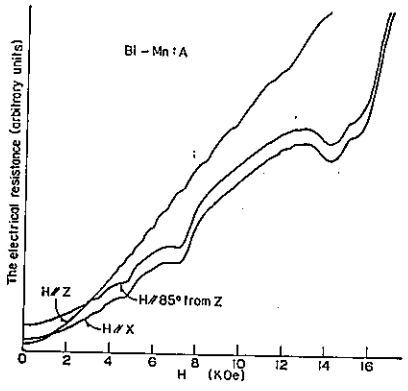

Fig. 17.

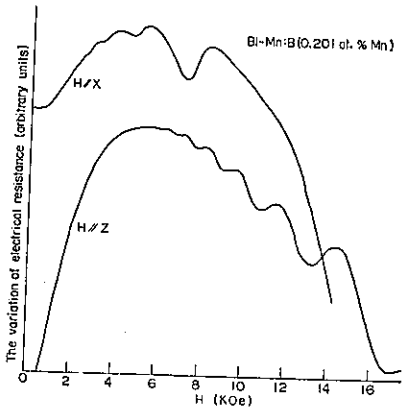

Fig. 18.

Fig. 17. The transverse magnetoresistance of the alloy Bi-Mn:A for H//x and H//z at 1.2°K.

Fig. 18. Shubnikov-de Haas oscillations of the alloy Bi-Mn:B for H//x and H//z at 1.2°K.

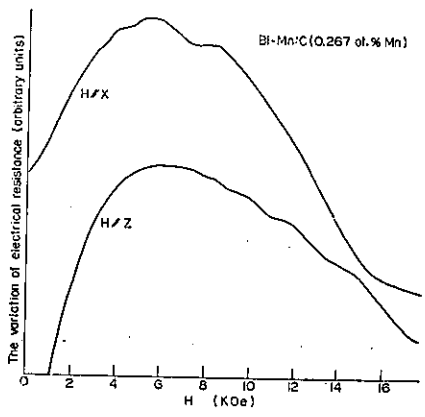

Fig. 19.

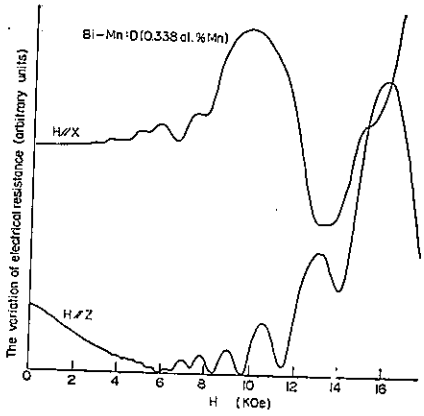

Fig. 20.

Fig. 19. Shubnikov-de Haas oscillations of the alloy Bi-Mn: C for H//x and H//z at 1.2°K.

Fig. 20. Shubnikov-de Haas oscillations of the alloy Bi-Mn: D for H//x and H//z at 1.2°K.

* The curve for the case in which the magnetic field was set 85° from the trigonal axis is also included. This curve is quite similar to the one in which the field was parallel to the binary axis. Both curves manifest the spin splitting due to electron.

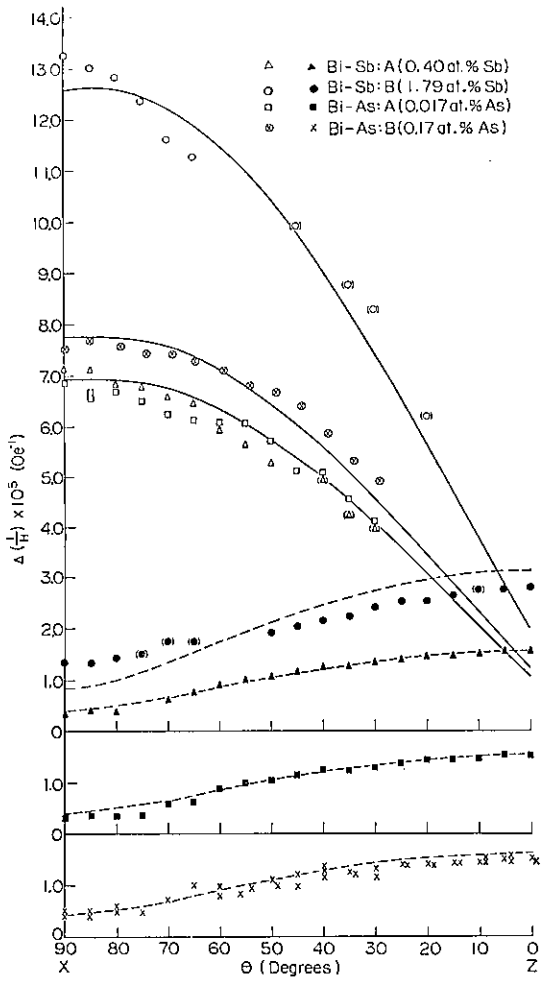

Fig. 21. Angular dependence of the periods observed in the Shubnikov-de Haas effect of Bi-Sb and Bi-As alloys.

de Haas oscillations of Bi-Mn: B, C, and D alloys, respectively. These characteristics are very similar to the case of the specimen Bi-Mn: A.

The relationships between the periods of the oscillations and the angle of the magnetic field, which are obtained from the above mentioned measurements, are shown in Fig. 21 for the Bi-As and the Bi-Sb alloys, in Fig. 22 for the Bi-Te and the Bi-Sn alloys, and in Fig. 23 for the Bi-Mn alloys.

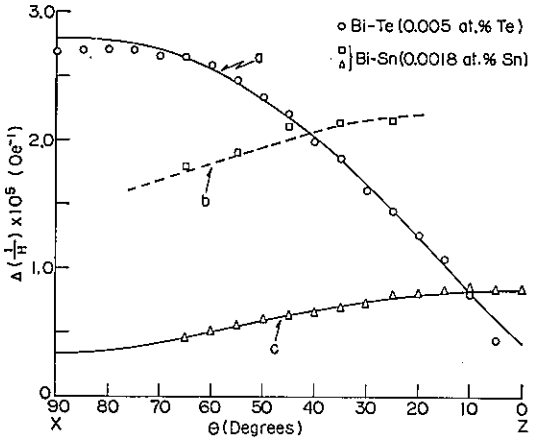

Fig. 22. Angular dependence of the periods observed in the Shubnikov-de Haas effect of Bi-Te and Bi-Sn alloys.

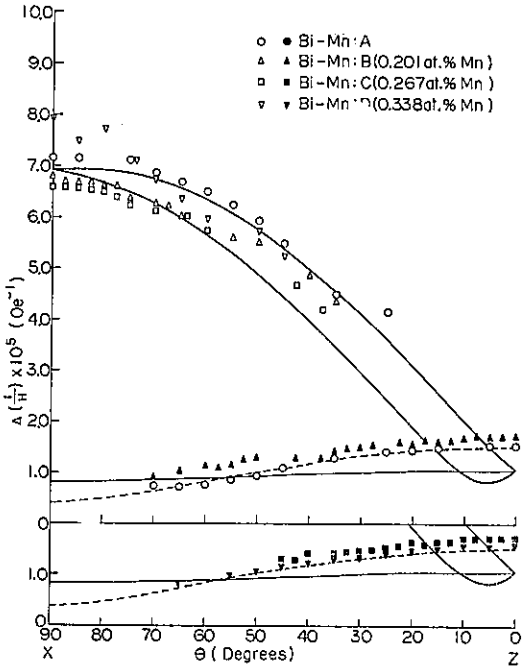

Fig. 23. Angular dependence of the periods observed in the Shubnikov-de Haas effect of Bi-Mn alloys.

IV. Discussion

The Fermi surfaces of electron and hole in bismuth were deduced experimentally by Shoenberg[13] and Brandt[14] and have been corroborated by many other investigators. The Fermi surfaces of electron are expressed by the following equations:

$$2m_0 E_{Fele.} = \alpha_{11} P_x^2 + \alpha_{22} P_y^2 + \alpha_{33} P_z^2 + 2\alpha_{23} P_y P_z , \tag{1,a}$$

$$2m_0 E_{Fele.} = \frac{1}{4}(\alpha_{11} + 3\alpha_{22}) P_x^2 + \frac{1}{4}(3\alpha_{11} + \alpha_{22}) P_y^2 + \alpha_{33} P_z^2 \pm \frac{\sqrt{3}}{2}(\alpha_{11} - \alpha_{22}) P_x P_y \pm \sqrt{3}\alpha_{23} P_z P_x - \alpha_{23} P_y P_z , \tag{1,b}$$

in which we denote the binary, bisectrix, and trigonal axes as x, y, and z axes, respectively, E_{Fele} and α_{ij} stand for the Fermi energy and the components of the reciprocal effective mass tensor of electron. The Fermi surface of hole is given by

$$2m_0 E_{Fhole} = \beta_{11}(P_x^2 + P_y^2) + \beta_{33} P_z^2 , \tag{1,c}$$

where E_{Fhole} and β_{ij} are the Fermi energy and the reciprocal mass parameter of hole. In addition, the components of the reciprocal effective mass parameter, α_{ij}, are defined by the next relations:

$$m_{11} = \frac{m_0}{\alpha_{11}} , \quad m_{22} = \frac{\alpha_{33} m_0}{\gamma} , \quad m_{33} = \frac{\alpha_{22} m_0}{\gamma}$$

$$m_{23} = -\frac{\alpha_{23} m_0}{\gamma} , \qquad (\gamma = \alpha_{22}\alpha_{33} - \alpha_{23}^2) . \tag{2}$$

Recently, however, the band structure of electron becomes more precisely elucidated in terms of its non-parabolicity[30,34,35].

According to Onsager[36], the period of the de Haas-van Alphen type oscillation for a general Fermi surface is given by

$$P_1 = \Delta\left(\frac{1}{H}\right) = \frac{eh}{cA_{ex}} . \tag{3}$$

where H is the magnetic field strength.

$$\Delta\left(\frac{1}{H}\right) = \frac{1}{H_i} - \frac{1}{H_{i+1}} ,$$

where H_i and H_{i+1} denote the magnetic field strength corresponding to the maximum or the minimum of successive oscillations. A_{ex} is the extreme cross-sectional area of the Fermi surface in momentum space perpendicular to the magnetic field. And e, h, and c have the conventional meanings. For the Fermi surface described in eq. (1), A_{ex} in eq. (3) can be calculated for each magnetic field direction. For the magnetic field H contained in y-z plane making an angle θ from z-axis, the periods are given as follows:

(34) B. Lax, Bull. Amer. Phys. Soc., **5** (1960), 167.
(35) M.H. Cohen, Phys. Rev., **121** (1961), 387.
(36) L. Onsager, Phil. Mag., **43** (1952), 1006, or See I.M. Lifshitz and A.M. Kosevich, Sov. Phys. J.E.T.P., **2** (1956), 636.

$$\Delta\left(\frac{1}{H}\right)_1 = \frac{e\hbar}{cm_0 E_F}\left[\alpha_{11}\alpha_{22}\cos^2\theta + \alpha_{11}\alpha_{33}\sin^2\theta - 2\alpha_{23}\alpha_{11}\sin\theta\cos\theta\right]^{1/2}, \quad (4,a)$$

$$\Delta\left(\frac{1}{H}\right)_{2,3} = \frac{e\hbar}{cm_0 E_F}\left[\alpha_{11}\alpha_{22}\cos^2\theta + \alpha_{23}\alpha_{11}\sin\theta\cos\theta + \frac{3(\alpha_{22}\alpha_{33} - \alpha_{23}^2) + \alpha_{33}\alpha_{11}}{4}\sin^2\theta\right]^{1/2}. \quad (4,b)$$

For H in the z-x plane at an angle θ from the z-axis, the periods become

$$\Delta\left(\frac{1}{H}\right)_1 = \frac{e\hbar}{cm_0 E_F}\left[\alpha_{11}\alpha_{22}\cos^2\theta + (\alpha_{22}\alpha_{33} - \alpha_{23}^2)^2\sin^2\theta\right]^{1/2}, \quad (5,a)$$

$$\Delta\left(\frac{1}{H}\right)_{2,3} = \frac{e\hbar}{cm_0 E_F}\left[\alpha_{11}\alpha_{22}\cos^2\theta \pm \sqrt{3}\,\alpha_{23}\alpha_{11}\sin\theta\cos\theta + \frac{(\alpha_{22}\alpha_{33} - \alpha_{23}^2) + 3\alpha_{11}\alpha_{22}}{4}\sin^2\theta\right]^{1/2}. \quad (5,b)$$

And for H in the x-y plane at an angle θ from the x-axis, the periods become

$$\Delta\left(\frac{1}{H}\right)_1 = \frac{e\hbar}{cm_0 E_F}\left[(\alpha_{22}\alpha_{33} - \alpha_{23}^2)\cos^2\theta + \alpha_{11}\alpha_{33}\sin^2\theta\right]^{1/2}, \quad (6,a)$$

$$\Delta\left(\frac{1}{H}\right)_{2,3} = \frac{e\hbar}{cm_0 E_F}\left[\frac{(\alpha_{22}\alpha_{33} - \alpha_{23}^2) + 3\alpha_{11}\alpha_{33}}{4}\cos^2\theta \pm \frac{\sqrt{3}}{2}(\alpha_{22}\alpha_{33} - \alpha_{23}^2 - \alpha_{11}\alpha_{33})\sin\theta\cos\theta + \frac{\alpha_{33}\alpha_{11} + 3(\alpha_{22}\alpha_{33} - \alpha_{23}^2)}{4}\sin^2\theta\right]^{1/2}. \quad (6,b)$$

In the magneto-acoustic attenuation measurements, the giant quantum oscillation as predicted by Gurevich, Skobov and Firsov[37] is observed under the condition of

$$E_F > \hbar\omega_c > kT \quad \text{and} \quad ql\left(\frac{\hbar\omega_c}{E_F}\right)^{1/2} \gg 1, \quad (7)$$

where E_F is the Fermi energy, ω_c the cyclotron frequency, q the wave number of the ultrasonic wave, l the mean free path of the charge carrier, and other symbols have the conventional meanings. The peaks of such giant type oscillation are really periodic in H^{-1} and the period is given by

$$P_2 = \frac{e\hbar}{cA_0} \quad (8)$$

From eqs. (3) and (8) we have

(37) V.L. Gurevich, V.G. Skobov and Y.A. Firsov, Sov. Phys. JETP, **13** (1961), 552.

$$\frac{P_2}{P_1} = \frac{A_{ex}}{A_0} \qquad (9)^*$$

If the angle between q and H is not too close to 90°, then for the most experimental situations A_0 is so close to A_{ex} that the period P_2 of the giant quantum oscillation is very near to the period P_1 of de Haas-van Alphen effect.

In the present experiment, the quantum oscillations, which are arised in the cases that the Landau levels cross the Fermi level, are observed by means of the de Haas-van Alphen effect, the magneto-acoustic attenuation, and the Shubnikov-de Haas effect for pure bismuth. As shown in Figs. 8, 9, and 10, the angular dependence of the periods of the quantum oscillations observed in the above-mentioned effects is quite similar to one another. The solid and dotted lines in these figures were drawn from the analysis of the observed values by means of eqs. (4), (5), and (6). This analysis gave simultaneously the effective mass parameters of the charge carrier, α_{ij} or β_{ij}, which are listed in Table 2 together with other

Table 2. The band parameters of pure bismuth

Band parameter	Aubrey et al.[25]	Galt et al.[26]	Brandt et al.[14]	Kao et al.[27,28]	Mase et al.[33]	Smith et al.[38]	Ours Ultrasonic	Ours Shubnikov-de Haas
α_{11}	202	114	192	141	192	192	206	121
α_{22}	1.67	1.39	1.58	1.53	1.64	1.24	1.56	2.24
α_{33}	83.3	108	79.0	86.3	81.1	73.2	80.9	121
α_{23}	8.33	9.47	8.42	9.01	9.41	5.49	8.78	10.2
$Ne(=3n_e)$			3.0×10^{17}	3.9×10^{17}	3.21×10^{17}	2.75×10^{17}	3.18×10^{17}	2.25×10^{17}
β_{11}		14.7	15.2	14.8	16.6	15.6	16.7	16.0
β_{22}		14.7	15.2	14.8	16.6	15.6	16.7	16.0
β_{33}		1.07	1.61	1.32	1.84	1.45	2.34	1.09
N_h			2.76×10^{17}	3.5×10^{17}	2.55×10^{17}	2.75×10^{17}	2.3×10^{17}	3.57×10^{17}

authors' values. Our values of α_{ij} and β_{ij} in each measurement are not exactly equal to one another but in fairly good agreement with other results[14,25-28,33,38]. The slight deviation of our results from others could be fairly modified by taking into account the misorientation of crystal axes within a few degrees.

Shubnikov-de Haas effect has also been studied in bismuth alloys doped with a small amount of tin, tellurium, manganese, antimony, and arsenic, respectively. The oscillatory behavior of each specimen is distinguished by the valence of the added minor element and the characteristic period of the oscillation can be understood in terms of the relative shift of the Fermi level to the conduction and the

(38) G.E. Smith, G.A. Baraff and J.M. Rowell, Phys. Rev., **135** (1964), A1118.

* The detailed explanation of eq. (9) should be referred to eq. (5) in the paper by Y. Shapira and B. Lax (Phys. Rev., **138** (1965), A 1191).

valence bands. It has been shown that tin and tellurium act as an acceptor and a donor, respectively, so that the Fermi level of bismuth moves upwards and downwards as the concentrations of tin and tellurium increase as displayed in Fig. 24.

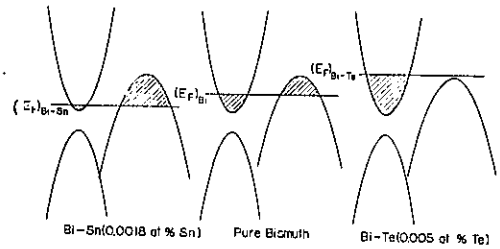

Fig. 24. The schematic diagram of the electronic band structure in Bi-Sn and Bi-Te alloys, showing the displacement of Fermi level in dilute bismuth alloys.

Under the assumption that the Fermi surface of electron is described by eq. (1) of a parabolic ellipsoidal model proposed by Shoenberg, the electron concentration in the conduction band is given by

$$n_e = \frac{8\pi}{2h^3} \cdot \frac{(2m_0 E_F)^{3/2}}{\sqrt{\alpha_{11}(\alpha_{22}\alpha_{33} - \alpha_{23}^2)}}, \tag{10}$$

where

$$\frac{m_0^{3/2}}{\sqrt{\alpha_{11}(\alpha_{22}\alpha_{33} - \alpha_{23}^2)}} = \sqrt{m_{11}(m_{22}m_{33} - m_{23}^2)}$$

On the other hand, by simplifying Cohen's non-ellipsoidal and non-parabolic model[28][35], one of the Fermi surfaces of electron can be expressed by

$$\frac{P_1^2}{2m_1} + \frac{P_2^2}{2m_2} + \frac{P_3^2}{2m_3} = E_F\left(1 + \frac{E_F}{E_g}\right) - \frac{1}{E_g}\left(\frac{P_2^2}{2m_2}\right)^2 \tag{11}$$

where 1, 2, and 3 refer to the principal axis system of the Fermi surface, the m's are the effective masses at the bottom of the conduction band, E_g is the energy gap, and E_F the Fermi energy. In this case the concentration of electron is given by

$$n_e = \frac{16\pi}{3h^3}(2m_1 m_2 m_3)^{1/2} E_F^{3/2}\left(1 + \frac{6}{5}\frac{E_F}{Eg}\right) \tag{12}$$

and E_g=0.0015 eV was obtained by Lax et al.[30] and the effective masses of electron at the bottom of the conduction band were given, say, by Kao et al.[28] as follows:

$$m_1 = 0.00163\, m_0\,, \quad m_2 = 1.35\, m_0\,, \quad m_3 = 0.00264\, m_0\,.$$

In the Bi-Sn alloy specimen (0.0018 at. % Sn) treated in the present experiment, the Fermi level is estimated to be located either 0.002 eV lower (by

the Shoenberg's model of eq. (1)) or 0.007 eV lower (by the Cohen's model of eq. (11)) than that of pure bismuth. While in the Bi-Te alloy specimen (0.005 at. % Te) studied here, the Fermi level is also estimated to be located either 0.018 eV higher (by the model of eq. (1)) or 0.02 eV higher (by the model of eq. (11)) than that of pure bismuth. It is generally admitted that the Fermi energy of hole is 0.012 eV and that of electron is 0.018 eV for pure bismuth. But when the non-parabolic electron band is assumed, the Fermi energy of electron is appraised at 0.025 eV. It is deduced from the above estimations in conformity with both models that only the conduction band gives rise to the oscillations in the case of Bi-Te alloy, while both of the conduction and the valence bands participate to the oscillatory effect in the case of Bi-Sn alloy. Accordingly, we can expect that the periods of the Shubnikov-de Haas oscillations observed in the case of Bi-Sn and Bi-Te alloys would be remarkably different from the case of pure bismuth. Our observed data are qualitatively explained in terms of the above consideration.

On comparing Fig. 22 with the data obtained when the magnetic field was rotated in the z-x plane in Fig. 10, it is reliable that the curve "*a*" in Fig. 22, which was observed in the Bi-Te alloy specimen, may correspond to the curve "*a*" in Fig. 10 due to electron in pure bismuth. This correspondence means that the addition of tellurium into bismuth gives rise to a decrease in the period of the Shubnikov-de Haas oscillation, that is to say, the cross-sectional area of the Fermi surface of electron in Bi-Te alloy becomes larger than that of pure bismuth. Similarly, it will be permitted that the curve "b" and "c" in Fig. 22, which were observed in the Bi-Sn alloy specimen, correspond to the curve "b" due to electron and the curve "c" due to hole of pure bismuth in Fig. 10. Then we can find that the period due to the conduction band increases and that due to the valence band decreases by the addition of tin into bismuth, that is to say, the cross-sectional area of the Fermi surface of electron in the Bi-Sn alloy specimen becomes smaller and that of hole becomes larger than those of the corresponding Fermi surface of pure bismuth. From the above experimental results, we can conclude that tin and tellurium act as an acceptor and a donor in bismuth, respectively, and give rise to a shift of the Fermi level of bismuth.

On the other hand, since antimony and arsenic belong to the same column in the periodic table as bismuth, the addition of antimony or arsenic to bismuth does not affect the characteristic property as semimetals, i.e. the condition that $N_h=N_e(=3n_e)$ is retained, where N_h and N_e denote the total number of hole and electron in unit volume, and n_e the number of electron per one ellipsoid in unit volume. The relative shift of the conduction and the valence bands as shown in Fig. 25, however, is expected with the increase of the concentration of antimony and arsenic. The former inference has been examined in terms of the H^2 depedence of the magnetoresistance in Bi-Sb[5] and Bi-As[7] alloys, and the latter fact has been elucidated from the appearance of semiconducting range in Bi-Sb system [5,31].

Since the Bi-As and Bi-Sb alloy specimens under study contain only a

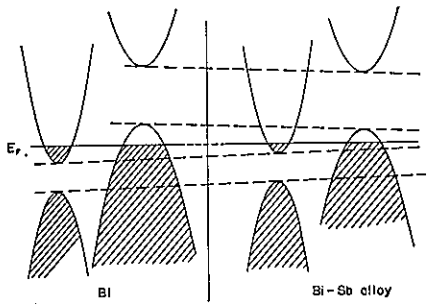

Fig. 25. The schematic diagram of the relative variation of the electronic band structure from Bi to Bi-Sb alloy, proposed by Tanuma.*)

small amount of arsenic or antimony, it is expected that the relative movement of the electronic band is very slight; hence the periods of the Shubnikov-de Haas oscillations are nearly equal to or slightly larger than that of pure bismuth. The present results shown in Fig. 21 are fairly explained in terms of the above consideration and may be concluded that the energy overlapping at the Fermi level decreases with the increase of the concentration of antimony or arsenic in bismuth.

From the result for the specimen Bi-Sb: B containing 1.79 at. % of antimony, we can deduce an interesting conclusion. That is to say, by comparing the periods due to electron and hole in the alloy specimen with those of pure bismuth, we obtain a scaling factor of 1.82 for electron and that of 2.04 for hole. Under the assumption of the parabolic electron band and the parabolic hole band, we have

$$\frac{P_{Bi-Sb}}{P_{Bi}} = \frac{(E_F)_{Bi}}{(E_F)_{Bi-Sb}} \begin{cases} = 2.04 & \text{for hole } (H//z)\,. \\ = 1.82 & \text{for electron } (H//z)\,. \end{cases} \tag{13}$$

so we can obtain $(E_{F\,hole})_{Bi-Sb}=0.0058$ eV as $(E_{F\,hole})_{Bi}=0.012$ eV and $(E_{F\,ele.})_{Bi-Sb}=0.0098$ eV as $(E_{F\,ele.})_{Bi}=0.018$ eV.

In general the parabolic ellipsoidal model is well known to a good approximation for the overlapping valence band, so that we obtain the hole concentration in the above mentioned alloy as $N_h=1.15\times10^{17}/\mathrm{cm}^3$. From the condition of $3n_e=N_h$, we have $n_e=0.38\times10^{17}/\mathrm{cm}^3$, which is the number of electron in the said alloy specimen. Then, we have $(E_{F\,ele.})_{Bi-Sb}=0.0015$ eV from eq. (10) for the parabolic ellipsoidal model using the effective mass obtained by Galt et al.[26]; while we have $(E_{F\,ele.})_{Bi-Sb}=0.014$ eV from eq. (12) for the non-parabolic non-ellipsoidal mdoel of eq. (11) with the effective mass obtained by Kao et al.[28] In another way, however, we can estimate $(E_{F\,ele.})_{Bi-Sb}=0.016$ eV for the non-parabolic non-ellipsoidal model by use of the next relationship:

*) S. Tanuma: Doctoral Thesis, Tohoku University, 1961. In Japanese.

$$\frac{P_{Bi-Sb}}{P_{Bi}} = \frac{(E_F)_{Bi}\left(1+\frac{(E_F)_{Bi}}{E_g}\right)^{1/2}}{(E_F)_{Bi-Sb}\left(1+\frac{(E_F)_{Bi-Sb}}{E_g}\right)^{1/2}} = 1.82 \qquad (14)$$

in which we used the values of $(E_F)_{Bi}$=0.025 eV., E_g=0.015 eV and that of the effective mass obtained by Kao et al.[28] In the final event, we obtain as the value of the Fermi energy of electron in the specimen Bi-Sb: B either 0.0098 eV or 0.0015 eV for the parabolic ellipsoidal model, and obtain either 0.016 eV or 0.014 eV for the non-parabolic non-ellipsoidal model. This calculation would lead us to prefer exclusively the Cohen's model as the electron band of bismuth.

A dilute alloying of transition metals, i.e. that of manganese offers us some interesting problems. The monotonic part of the transverse magnetoresistance in bismuth alloys containing a few tens % of manganese continues to increase to a high magnetic field[32]. This result tells us that one of the most essential condition for semimetals, i.e. $N_e \sim N_h$, is also fulfilled in Bi-Mn alloys, that is to say, manganese atom acts as neither an acceptor nor a doner in bismuth. Accordingly, the periods of the oscillation of Shubnikov-de Haas effect in Bi-Mn alloys are much the same as in pure bismuth, as shown in Fig. 23. Another property of manganese as an impurity lies in the fact that manganese atom gives no localized moment in bismuth[32]. This is the most different nature of the dilute Bi-Mn alloys from other kinds of alloys containing a small amount of manganese, say, Cu-Mn, Zn-Mn and others.

Summary

We have studied the electronic band structure of bismuth and its alloys by means of the de Haas-van Alphen effect, the magneto-acoustic effect, and the Shubnikov-de Haas effect. Our results for pure bismuth was in good agreement with the results by many other investigators.

The results for dilute bismuth alloys could be illustrated in terms of the relative shift of the Fermi level with respect to the conduction and valence bands of bismuth. Especially, the result of the specimen Bi-Sb: B highly-doped with 1.79 at. % antimony led us to prefer the Cohen's model for the conduction band of bismuth.

Manganese atom acts as a neutral impurity in bismuth, which donates neither electron nor hole to the band of bismuth. Furthermore, it could be concluded that manganese shows no localized moment in bismuth.

Acknowledgements

The authors would like to express their sincere thanks to Prof. S. Tanuma, University of Tokyo, and to Prof. S. Mase, Kyushu University, for many enlighte-

ning discussions during the present study. The authors would like to express thanks to Mr. Tsuneo Miura of the Pure Metals Service Center in this Institute for his help in preparing single crystals of pure bismuth. Thanks are also due to Mr. H. Kitagawa and Mr. M. Hongo for their helps in performing the experiments.